

A fundamental theory for the range fluctuations of 10^{12}eV to 10^{18}eV muons in water based on *Time Sequential Procedure*

Y.Okumura^a, N.Takahashi^a, A.Misaki^{b,c}

^aGraduate School of Science and Technology Hirosaki University, Hirosaki, 036-8561, Japan

^bInnovative Research Organization, Saitama University, Saitama, 338-8570, Japan

^cThe Institute for China-Japan Culture Study, Mitaka, Tokyo, 113-0004, Japan

Abstract

In 1983 to 84, we proposed a new method in which all stochastic processes concerned are exactly taken into account as for range fluctuation of high energy muons, without introducing any approximation which may distort fluctuation effect. Now, we call it tentatively *Time Sequential Procedure*. In 1991, Lipari and Stanev proposed another method for the same problem. They divided the problem into two part, *soft part* and *hard part*, and applied Monte Carlo technique to the latter part. Here, we call their method tentatively *V_{cut} Procedure*. It is well known that the procedure has been widely utilized in the analysis of high energy muon events in KM3 detectors. In the present paper, we examine the limit for applicability to *V_{cut} Procedure* for the range fluctuation, comparing with *Time Sequential Procedure*. It is concluded that *V_{cut} Procedure* give not so different values from *Time Sequential Procedure* on the survival probability for high energy muons, but it connotes critical problems related to energy measurements on high energy muon events due to Cherenkov light signals, owing to the inconsistency of the procedure involved. Thus, we try to the revival of *Time Sequential Procedure* for the establishment of more reliable theory for the observation of Cherenkov light whose origins are high and extremely high energy muons.

Keywords: High energy muon, Muon range fluctuation, Muon energy loss, Muon propagation simulation

1. Introduction

The studies on depth intensity problem of high energy muons have been one of the most important subjects in traditional cosmic ray physics, relating to elucidation on unknown character of high energy cosmic ray muons, and still have never been lost its importance. Menon and Ramana Murthy [1] wrote an excellent review on this subject at greater depths which describes from the first experiment carried out Simizu tunnel in Japan (1940-1945) [2] to the last experiment related to the neutrino carried out in Kolar Gold Mine, India (Up to 1964) [3]. Bugaev et al. [4] have discussed this problem related to the charm production mechanism, adding new data, from, such as, DUMAND, Baikal, MACRO, LVD, NESTOR and others up to 1977. Now, the gigantic projects for neutrino astrophysics called as KM3 detectors are now being developed in the lake [5], Antarctic [6] and Ocean [7,8]. In the analysis of these KM3 detectors, the depth intensity relation

for high energy muon is utilized for the confirmation of their experimental reliabilities related to other experiments different depths [5-8].

The theories of range fluctuation of high energy muons are indispensable means in the analysis of the depth intensity relation of high energy muons at certain depths. The theories of range fluctuation are studied in three different manners. The first one is analytical manner [9-19], the second one is numerical one [20] and the third one the Monte Carlo manner [21-34].

At the same time, the theories of range fluctuation of high energy muons offer essential tools for energy determination of high energy muon events from neutrino interactions in KM3 detectors. Their energies, in particular higher energies, are estimated from Cherenkov light signals from muon induced electromagnetic cascade showers, not rather than from muons themselves, but, in spite of this situation, examination of behaviors of muons themselves are essentially important, because they are

origins of electromagnetic cascade showers from different modes of interactions due to muons.

At present time, studies on the fluctuation of high energy muons have been made by the Monte Carlo method, using electronic computers with great performance, because only this method can clarify fluctuation characters of muons correctly, while analytical method and numerical one provide essentially their average behavior. The detailed studies around fluctuation of high energy muon events are inevitable, owing to small number of physical events concerned in addition to sharp steepness of the parent neutrino energy spectrum which are the origin of fluctuation. The studies on the range fluctuation of high energy muons by Monte Carlo method had been made even before appearance of electronic computer with great performance [21-25]. However, then, they were forced to put more simplified, even more artificially assumptions on their stochastic processes concerned for saving both man powers and computer ones at the period for computation.

In 1983 to 84, Takahashi et al. [26,27] had developed a new Monte Carlo technique where every stochastic process for high energy muon concerned is treated exactly from the stochastic point of view. Namely, the interaction points and the energy division due to interactions concerned (bremsstrahlung, direct electron pair production and photonuclear interaction) are exactly treated in stochastic manner. In the present paper, we call it tentatively *Time Sequential Procedure*.

In 1991, Lipari and Stanev [28] developed another technique, from a point of the philosophy of Monte Carlo method. They put the diffusion equation on the fluctuation in the form of differential-integral equation and solve it by Monte Carlo technique. They divided the part which is the origin of fluctuation into two parts, namely, *hard part* (radiation loss part) and *soft part* (continuous energy loss part). In radiation loss part only, they treat fluctuation in Monte Carlo way, but in *soft part* they approximate fluctuation as continuous energy loss, supposing small effect of fluctuation. This technique has been adopted by subsequent authors [29-34]. In the present paper, we call it tentatively *V_{cut} Procedure*. Now, *V_{cut} Procedure* [28-34] has been extensively utilized in the analysis of muon neutrino events KM3 detectors [for example, 6].

However, in our opinion, taking into account of the fact that Cherenkov light signal due to high energy muons mostly come from the muon induced electromagnetic cascade showers whose origins ei-

ther bremsstrahlung or direct electron pair production or photonuclear interaction, not from muons themselves in KM3 detector, the energy determinations of high energy muon events inevitably include more ambiguity in the case of *V_{cut} Procedure*, compared with the case of *Time Sequential Procedure* (see, the section 3 and Conclusion and Outlook).

In the present paper, we try to revitalize *Time Sequential Procedure* in 1993 for the more accurate analysis of high energy muon events in KM3 detector, comparing to the results obtained by *V_{cut} Procedure* which has been well distributed. Here, we restrict our concern to the fundamental and its application will be reported in subsequent papers.

2. Fundamental Structure of *Time Sequential Procedure*

Here, in order to clarify characteristics of *Time Sequential Procedure* in contrast to *V_{cut} Procedure*, we reproduce our procedure which had already been published in 1984 (in Japanese) [27].

2.1. The mean free paths for stochastic processes and their resultant mean free path

Behaviors of high energy muons are stochastically determined from elementary processes of bremsstrahlung [35], direct electron pair production [36] and photonuclear interaction processes [37]. Our idea is very simple and fundamental.

We treat these processes as stochastic ones as exactly as possible, without introducing any approximation in the energy region in which we are interested¹. In our program, these stochastic processes are prepared as subroutines and, therefore, they are easily replaced by the most advanced ones, if necessary keeping exactness of our logical structure.

Let us denote, differential cross sections for bremsstrahlung, direct electron pair production, and photonuclear interaction, $\sigma_b(E, E_b) dE_b$, $\sigma_d(E, E_d) dE_d$ and $\sigma_n(E, E_n) dE_n$, respectively. Here, E denotes the energy of muon concerned, E_b , the energy of γ -ray due to bremsstrahlung, E_d , the energy of electron pair due to direct electron pair production, E_n , the energy of emitted particles due to photonuclear interaction, respectively. Then, the

¹We adopt the minimum energy of muon for observation as 1 GeV throughout paper. Namely, the behaviors of muons with larger than 1 GeV are exactly described, following the stochastic probability functions concerned.

mean free paths for different stochastic processes are energy dependent of the muon concerned and they are given as follows: For bremsstrahlung processes,

$$\lambda_b(E) = \frac{1}{\frac{N}{A} \int_{E_{b,min}}^{E_{b,max}} \sigma_b(E, E_b) dE_b} \quad (1)$$

Here, $E_{b,min}$ is taken in such a way that $E_{b,min}/E$ is sufficiently smaller than E_{min}/E . Here, E_{min} denotes the minimum energy of the muon for observation. E_{min} is taken as 1 GeV throughout present paper². The integrations for direct electron pair production and photonuclear interaction are performed over kinematically allowable ranges. For direct electron pair production processes,

$$\lambda_d(E) = \frac{1}{\frac{N}{A} \int_{E_{d,min}}^{E_{d,max}} \sigma_d(E, E_d) dE_d} \quad (2)$$

For photonuclear interaction processes,

$$\lambda_n(E) = \frac{1}{\frac{N}{A} \int_{E_{n,min}}^{E_{n,max}} \sigma_n(E, E_n) dE_n} \quad (3)$$

, where N and A denote Avogadro number and atomic mass number, respectively.

Also, $\lambda_{total}(E)$, the resultant mean free path for these stochastic processes are given as,

$$\frac{1}{\lambda_{total}(E)} = \frac{1}{\lambda_b(E)} + \frac{1}{\lambda_d(E)} + \frac{1}{\lambda_n(E)} \quad (4)$$

2.2. Determination of the kind of the stochastic processes and the real free path for the stochastic processes concerned

By using Eq. (1) to (4), we can determine the interaction points of muons for different stochastic processes in the following. The first, for the purpose, let us define $\xi_b(E)$ and $\xi_d(E)$ as follows;

$$\xi_b(E) = \frac{1/\lambda_b(E)}{1/\lambda_{total}(E)} \quad (5)$$

$$\xi_d(E) = \frac{1/\lambda_b(E) + 1/\lambda_d(E)}{1/\lambda_{total}(E)} \quad (6)$$

²Such the limitation is absolutely necessary for the exact treatment γ -rays due to bremsstrahlung in the energy region where we are interested owing to the infrared catastrophic characteristics of bremsstrahlung. In the present paper, the behavior of muons with energies larger than 1 GeV related to bremsstrahlung are exactly treated in stochastic manner, as well as those for direct electron pair production and photonuclear interaction.

The second, we sample randomly ξ_1 , a uniform random number between (0,1). If $\xi_1 \leq \xi_b(E)$, then we recognize the interaction occurs due to bremsstrahlung. If $\xi_b(E) < \xi_1 \leq \xi_d(E)$, then we understand the direct electron pair production occurs. If $\xi_1 > \xi_d(E)$, then, we understand that photonuclear interaction occurs.

Again, we sample a new ξ_2 , randomly from uniform random number between (0,1). Then, we can determine the interaction points Δt for the specified stochastic processes according the following criterion. In the case of the occurrence of bremsstrahlung processes (for $\xi_1 \leq \xi_b(E)$),

$$\Delta t_b = -\lambda_{total}(E) \log \xi_2 \quad (7)$$

In the case of the occurrence of direct electron pair production processes (for $\xi_b(E) < \xi_1 \leq \xi_d(E)$),

$$\Delta t_d = -\lambda_{total}(E) \log \xi_2 \quad (8)$$

In the case of the occurrence of photonuclear interaction processes (for $\xi_1 > \xi_d(E)$)

$$\Delta t_n = -\lambda_{total}(E) \log \xi_2 \quad (9)$$

We are taken into account of ionization loss addition to stochastic energy losses, by using Tamura's method [38].

2.3. Determination of the emitted energy loss (E_b or E_d or E_n) from the specified stochastic processes

Under the determination of the interaction points due to the specified stochastic processes, by using ξ_1 and ξ_2 , in the previous subsection, here, the energy losses E_b , E_d and E_n from the specified stochastic processes are given as follows. For sampled ξ_3 which is obtained randomly from the uniform random number between (0,1), we solve the following equations for respective interactions in order to obtain E_b or E_d or E_n . For bremsstrahlung process,

$$\xi_3 = \frac{\int_{E_{b,min}}^{E_b} \sigma_b(E, E_b) dE_b}{\int_{E_{b,min}}^{E_{b,max}} \sigma_b(E, E_b) dE_b} \quad (10)$$

For direct electron pair production,

$$\xi_3 = \frac{\int_{E_{d,min}}^{E_d} \sigma_d(E, E_d) dE_d}{\int_{E_{d,min}}^{E_{d,max}} \sigma_d(E, E_d) dE_d} \quad (11)$$

For photonuclear interaction,

$$\xi_3 = \frac{\int_{E_{n,min}}^{E_n} \sigma_n(E, E_n) dE_n}{\int_{E_{n,min}}^{E_{n,max}} \sigma_n(E, E_n) dE_n} \quad (12)$$

In Eq. (10) to (12) for respective interaction, the quantities to be obtained are $E_{b,d,n}$, emitted energy losses for given E , energy of the muon concerned. The quantities of $E_{b,d,n}$ are extended to $E_{b,d,n,min}$ to $E_{b,d,n,max}$. For sampled ξ_3 we can solve these equation numerically and obtain $E_{b,d,n}$ finally. Thus, we can determine $E_{b,d,n}$, the energy losses for the specified stochastic process at determined interaction point. A flow chart for the fundamental structure of *Time Sequential Procedure* is given Fig.1.

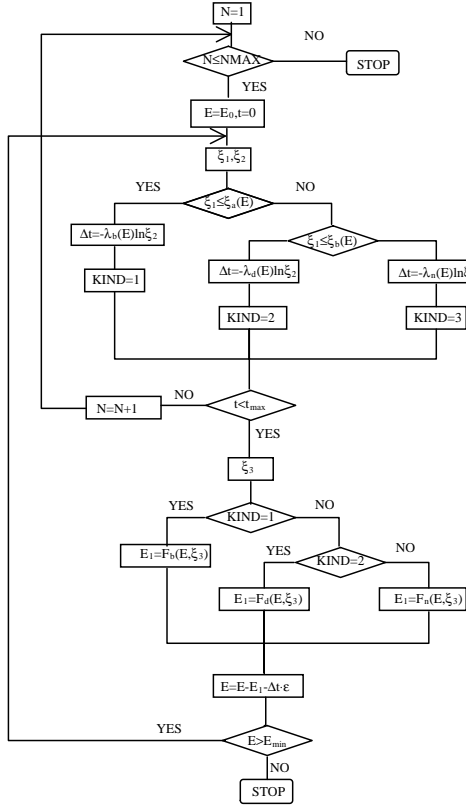


Figure 1: Flow Chart for the fundamental structure of *Time Sequential Procedure*.

2.4. On the validity of *Time Sequential Procedure*

Generally speaking, the verification of the validity of the Monte Carlo method concerned is pretty difficult. For the purpose, it is desirable to compare the physical results obtained by *Time Sequential Procedure* with the corresponding results obtained

by the analytical method which is methodologically independent of the Monte Carlo method concerned.

Once, Misaki and Nishimura [17] had developed an analytical theory for range fluctuation of high energy cosmic ray muons based on the Nishimura-Kamata formalism on electron shower theory to apply to study depth intensity relation muon underground. Takahashi et al. [26,27] had compared the depth dependence of the average energies of muons under the incident energy spectrum of the muons on the surface with the different indices ($\gamma = 2, 3$, and 4) obtained the analytical theory [17] with the corresponding quantities obtained by *Time Sequential Procedure*.

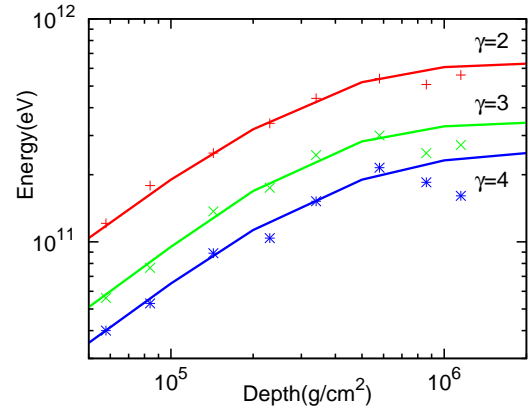


Figure 2: The average energies of the muons. The lines denote Misaki and Nishimura, while symbols ours.

We reproduce them in Fig.2 from the previous work [27]. The agreement between them is quite well, taking into account of the difference in both the cross sections concerned and their numerical evaluation method. Namely, we can say the logical structure of *Time Sequential Procedure* on the validity of is well established from the point of the validity of Monte Carlo method concerned.

2.5. Examples directly derived by the *Time Sequential Procedure*

2.5.1. The diversity of individual muon behavior 'Needle' structure of the energy losses from high energy muons

In subsections 2.2 and 2.3, by random sampling procedure, we show how to determine both interaction points for the specified stochastic processes and subsequent their energy losses for the interactions concerned. In the present subsections, we

show some examples of the energy losses along the passage of the high energy muons.

In Fig.3 to Fig.13, we show three different categories of the 'Needle' structure of the energy losses for the same primary energies. 'Needles' denote fractional energy losses due to a specified stochastic process such as, bremsstrahlung, direct electron pair production or photonuclear interaction at respective interaction points. We illustrate several typical structures of the energy loss of muons which start, having primary energy E_0 and reaching E_{min} , namely, the behaviors with the shortest range, with *the longest range* and with *the average-like range* for the same primary energy and the same starting point. *The shortest range* denotes the muon with the shortest range among all sampled muons, while *the longest range* does the muon with *the longest range* among all sampled muons, and *the average-like range* does the muon with the range whose is the nearest to the averaged range among all sampled muons. Total sampling numbers per respective primary energy are 100,000.

In these figures, we can recognize the diversities of muon behaviors for the same primary muon energies with regard to their ranges (or their energy losses). All interaction points due to the processes of bremsstrahlung, direct electron pair production and photonuclear interaction and all energy losses due to these elementary processes at respective points due to these processes are recorded. In order to clarify the diversities among the real range distributions (or real energy loss distributions), we examine the muons with *the shortest range*, the muons with *the longest range* and the muons with *the average-like range* in more detail.

In Table 1, we show numerically the characteristics of an individual muon with *the shortest range*, *the average-like range*, *the longest range*, in addition to their average range for 10^{12}eV , 10^{15}eV and 10^{18}eV .

In Fig.3 to Fig.5, we give the characteristic behaviors with *the shortest range*, *the average-like range* and *the longest range*, that is, their energy loss for the specified interaction as the function of the depth traversed for the primary energy of 10^{12}eV in water³. In these figures, we utilize the same scale in depth to clarify the diverse behav-

iors by the same incident energies, namely, those with *the shortest range*, with *the average-like range* and with *the longest range*, respectively. In figures, the abscissa denotes the depths where the specified interactions occur. The 'needles' (expressed in ordinate) with different colors at different depths denote ratios of the energy losses due to direct electron pair production (green, **d**), bremsstrahlung (red, **b**) and photonuclear interaction (blue, **n**) to their primary energy, respectively. The abrupt changes in them are due to the catastrophic energy losses for muons (see, footnote 2). It is easily understood that one sees the fluctuation effect rather weak in the energy of 10^{12}eV .

It is seen from figures and Table 1 that there is not so big difference between the case with *the shortest range* and one with *the longest range* for 10^{12}eV . In the case with *the shortest range* (Fig.3), we find two catastrophic energy losses (at ~ 910 meters and ~ 1870 meters) due to two bremsstrahlungs play the important role in the range. In the case with *the average-like range* (Fig.4), we can find one catastrophic energy loss due to bremsstrahlung at ~ 1.48 kilometer. However, in the case of *the longest range* (Fig.5), we cannot find the catastrophic energy losses due to bremsstrahlung and, instead, we can find that almost energy losses are due to many number (~ 300) of direct electron pair production events.

In Fig.7 to Fig.9, we give the typical diversities for primary energy of 10^{15}eV similarly for primary energy of 10^{12}eV . In these figures, the diversities for *the shortest range*, *the average-like range* and *the longest range* are compared explicitly expressed in the same scale. Fig.6 shows the same in Fig.7 in extended scale. Combined with Table 1, *the shortest range*, ~ 940 meter (Fig.6), is far shorter compared with *the longest range*, ~ 35.0 kilometers (Fig.9). It is seen from Fig.6 and the Table 1 that bremsstrahlung plays a decisive role as the cause of catastrophic energy loss in the case of *the shortest range*, ($\sim 96.5\%$ of total energy up to ~ 450 meters). 86.6% of the total energy is lost by 2 bremsstrahlungs, 13.4% by 367 direct electron pair productions and $5.9 \times 10^{-3}\%$ by 1 photonuclear interaction. In Fig.9, we give the case for *the longest range*. Here, large numbers of direct electron pair production with rather small energy loss play an important role, as shown similarly in Fig.5. Here, 80.2% of the total energy is lost by 13722 direct electron pair productions, 7.53% by 71 bremsstrahlungs and 11.1% by 105 photonuclear in-

³In order to understand the situation visually the characteristic behaviors of high energy muons which are shown Fig.3 to Fig.13, we suggest the readers to look at the pictures with colors in the WEB page.

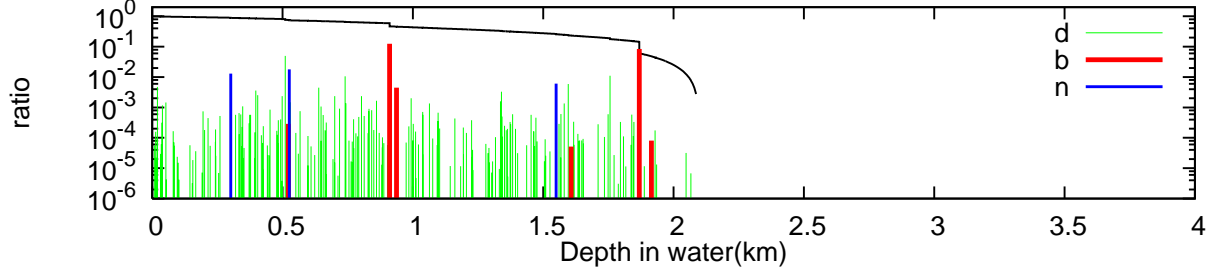


Figure 3: The fractional energy loss with *the shortest range* as the function of the depth for 10^{12} eV muon. A line graph in the upper denotes fractional muon energy as the function of the depth. [b] denotes the fractional energy loss due to bremsstrahlung, [d] due to direct electron pair production and [n] due to photonuclear interaction. [b], [d] and [n] are utilized as the same meaning up to Figure 13.

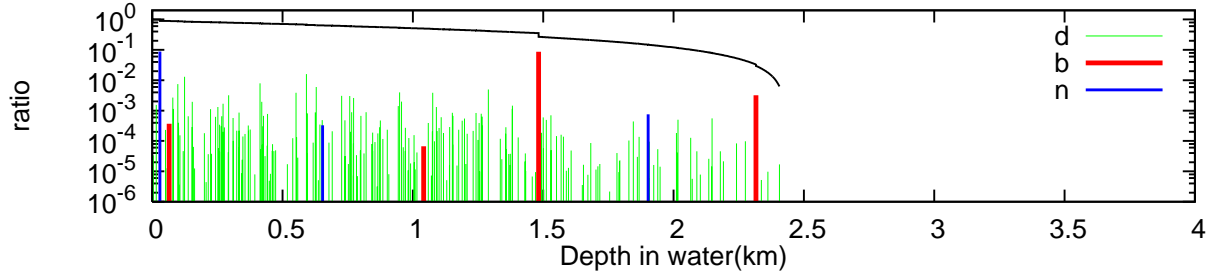


Figure 4: The fractional energy loss with *the average-like range* for 10^{12} eV muon together with the fractional energy of the muon.

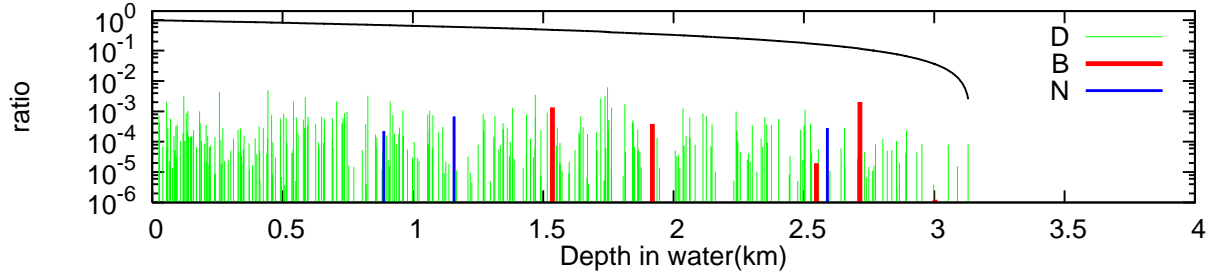


Figure 5: The fractional energy loss with *the longest range* for 10^{12} eV muon together with the fractional energy of the muon.

teractions. In Fig.8, combined with Table 1, we give the case with *the average-like range*. Here, 23.5% of the total energy is lost by 5489 direct electron pair productions, 75.0% by 49 bremsstrahlungs and 0.93% by 37 photonuclear interactions, while in the real averages (100,000 samples), 47.4% of the total energy is lost by 6800 direct electron pair productions, 35.3% by 48.1 bremsstrahlungs and 16.7% by 55.0 photonuclear interactions.

In Fig.10 to Fig.13, combined with Table 1, we show the similar relations for 10^{18} eV muons as shown in 10^{15} eV. We can say the case with *the shortest range* in Fig.10 (or Fig.11) has a strong

contrast to that with *the longest range*. The manner of the energy loss in Fig.10 is drastic with two big catastrophic energy losses due to bremsstrahlungs (~ 0.8 km and 4.74 km), while that in Fig.13 is very moderate with no catastrophic energy loss. *The shortest range*, ~ 7.7 kilometers (Fig.11), is far shorter compared with *the longest range*, ~ 57.8 kilometers (Fig.13). It is seen from Fig.10 and Table 1 in the case of *the shortest range* that bremsstrahlung plays a decisive role as the cause of catastrophic energy loss. 87.5% of the total energy is lost by 28 bremsstrahlungs, 11.9% by 5760 direct electron pair productions and 0.623% by 40

Table 1: The details of the characteristics on the muons with *the shortest range, the average-like range, the longest range and the average range.*

$E_0 = 10^{12} \text{ eV}$	Range [km]	Energy loss by brems[eV]	Number of interaction	Energy loss by direct pair[eV]	Number of interaction	Energy loss by nuclear[eV]	Number of interaction
<Average>	2.43	1.10×10^{11}	4.74	1.57×10^{11}	243	4.54×10^{10}	3.44
Average-like	2.43	8.97×10^{10}	4	1.34×10^{11}	221	8.86×10^{10}	3
Shortest	2.09	2.15×10^{11}	6	1.52×10^{11}	208	3.72×10^{10}	3
Longest	3.14	3.80×10^9	5	1.04×10^{11}	299	1.19×10^9	3
$E_0 = 10^{15} \text{ eV}$							
<Average>	1.78×10^1	3.53×10^{14}	48.1	4.74×10^{14}	6.80×10^3	1.67×10^{14}	55
Average-like	1.78×10^1	7.50×10^{14}	49	2.35×10^{14}	5489	9.31×10^{12}	37
Shortest	9.44×10^{-1}	8.66×10^{14}	2	1.34×10^{14}	367	5.90×10^{10}	1
Longest	3.50×10^1	7.53×10^{13}	71	8.02×10^{14}	13722	1.11×10^{14}	105
$E_0 = 10^{18} \text{ eV}$							
<Average>	3.28×10^1	3.37×10^{17}	108	4.39×10^{17}	2.57×10^4	2.25×10^{17}	172
Average-like	3.28×10^1	1.68×10^{17}	118	5.58×10^{17}	29321	2.74×10^{17}	196
Shortest	7.72×10^0	8.75×10^{17}	28	1.19×10^{17}	5760	6.23×10^{15}	40
Longest	5.78×10^1	5.71×10^{16}	162	5.77×10^{17}	46542	3.66×10^{17}	277

photonuclear interactions. In Fig.13, we give the case with *the longest range*. Here, 57.7% of the total energy is lost by 46542 direct electron pair productions, 36.6% by 277 photonuclear interactions and only 5.71% by 162 bremsstrahlungs in the complete absence of catastrophic energy losses. In Fig.12, we give the case with *the average-like range*. Here, 55.8% of the total energy is lost by 29321 direct electron pair productions, 16.8% by 118 bremsstrahlungs and 27.4% by 196 photonuclear interactions, while, in the real averages (100,000 samples), 43.9% of the total energy is lost by 2.57×10^4 direct electron pair productions, 33.7% by 108 bremsstrahlungs and 22.5% by 172 photonuclear interactions. Thus, it can be concluded that the diversity among muon propagation with the same primary energy should be noticed.

2.5.2. Average characteristics of high energy muons with the shortest range, the average-like range, the longest range around the average range

In Table 2 (a), we give the ratios of energy losses due to respective stochastic processes to total energy loss in the typical ranges (*the average, the average-like, the shortest and the longest*) for 10^{12} eV , 10^{15} eV and 10^{18} eV . It is clear from the table that, averagely speaking, high energy muons are lost $\sim 50\%$ in the direct electron pair production, $\sim 30\%$ in bremsstrahlung and $\sim 20\%$ in photonuclear

clear interaction. It is clear from Table 2(a) that the muon with the longest range loses $\sim 70\%$ in direct electron pair productions, in long chain of electron pairs induced electromagnetic cascade showers with rather smaller energies, while the muon with the shortest range loses $\sim 70\%$ to 100% of their energy in a few number of bremsstrahlungs (catastrophic energy loss).

In Table 2(b), the ratios of fractional energy loss for specified stochastic processes are divided by the corresponding averaged ones. It is clear from the Table 2(b) that the divisions of energy loss to the specified processes in *the average-like range* are clearly different from that of the averaged. It shows that the energy divisions for different processes are different, even if the ranges are same. This fact makes the ejection of the Cherenkov light influence, even if the paths of the high energy muons are same.

In Table 2(b), it is also clear from the characteristics of the typical showers from the point of energy dissipation that energy losses ratios of showers concerned to their averages due to bremsstrahlung in *the shortest ranges* lose their energies are 2.96, 2.53, 2.17 for primaries 10^{12} eV , 10^{15} eV and 10^{18} eV , respectively. Namely, these showers with *the shortest range* essentially lose their energies almost due to bremsstrahlung, while the corresponding ratios due to direct electron pair production in the showers with *the longest range* are 1.33, 1.52, 1.49. Also, these showers with *the longest range* lose their

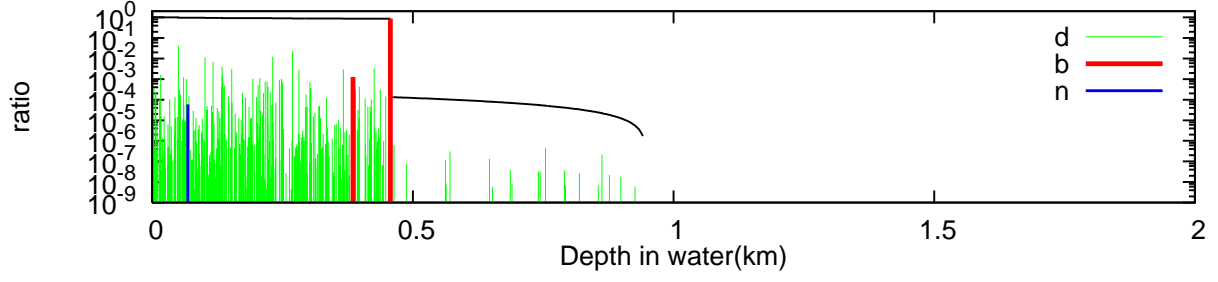


Figure 6: The fractional energy loss with *the shortest range* for 10^{15} eV muon together with the fractional energy of the muon. The figure is a magnification of Figure 7.

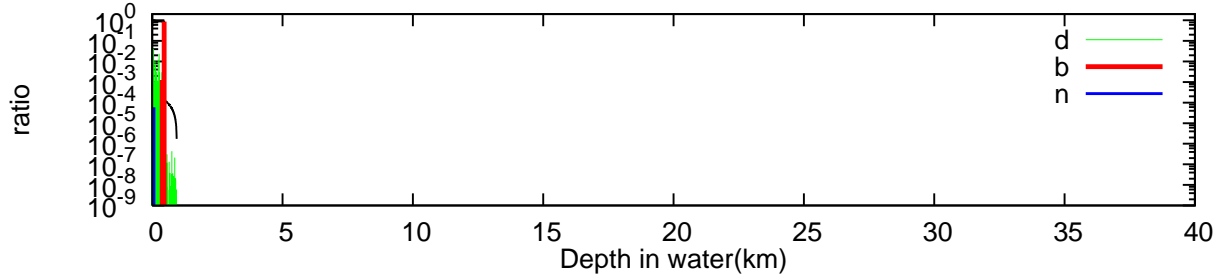


Figure 7: The fractional energy loss with *the shortest range* for 10^{15} eV muon together with the fractional energy of the muon.

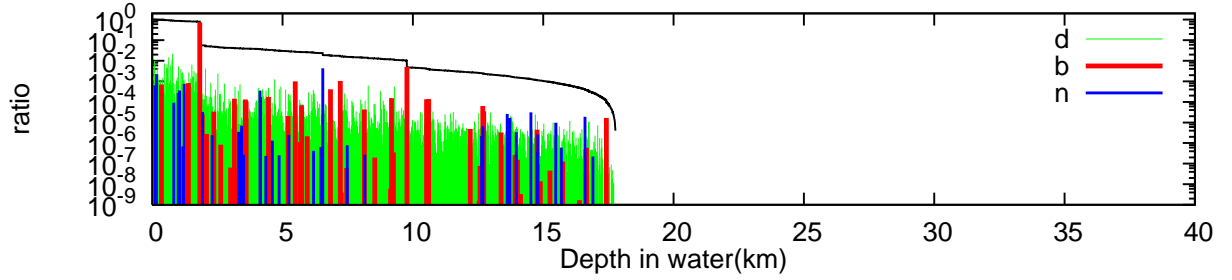


Figure 8: The fractional energy loss with *the average-like range* for 10^{15} eV muon together with the muon energy.

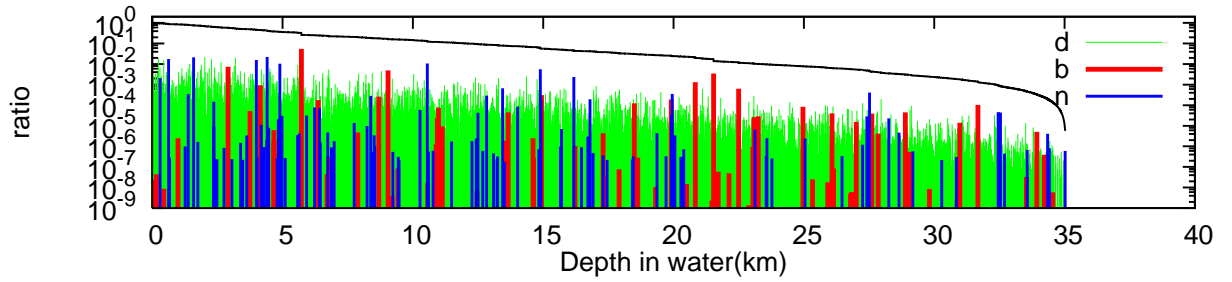


Figure 9: The fractional energy loss with *the longest range* for 10^{15} eV muon together with the fractional energy of the muon.

pretty energies owing to direct electron pair production.

2.5.3. Range Distributions and Hypothetical Range Distributions for high energy muons

As shown, for example, in Fig.3 to Fig.13, we can pursue three kinds of the typical types of the behaviors of high energy muons with definite pri-

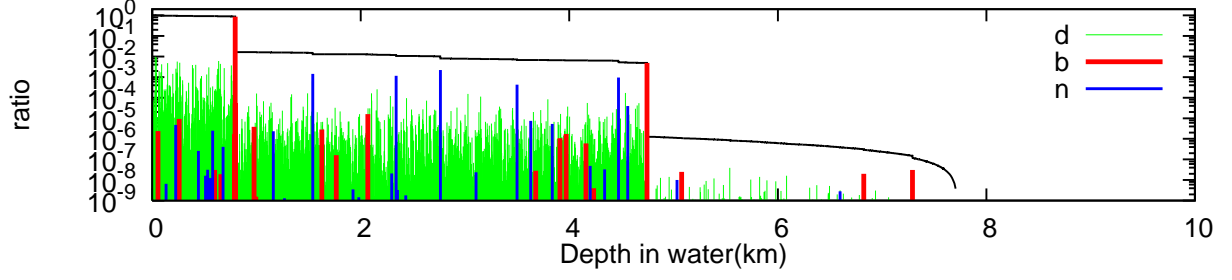


Figure 10: The fractional energy loss with *the shortest range* for 10^{18} eV together with fractional energy of the muon. The figure is a magnification of Figure 11.

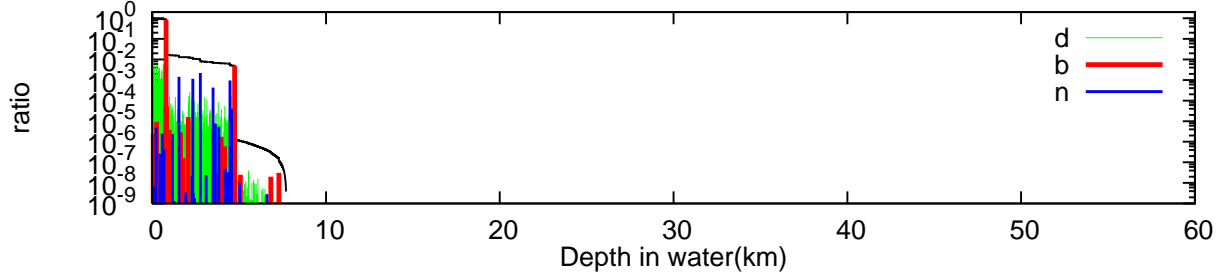


Figure 11: The fractional energy loss with *the shortest range* for 10^{18} eV muon together with the fractional energy of the muon.

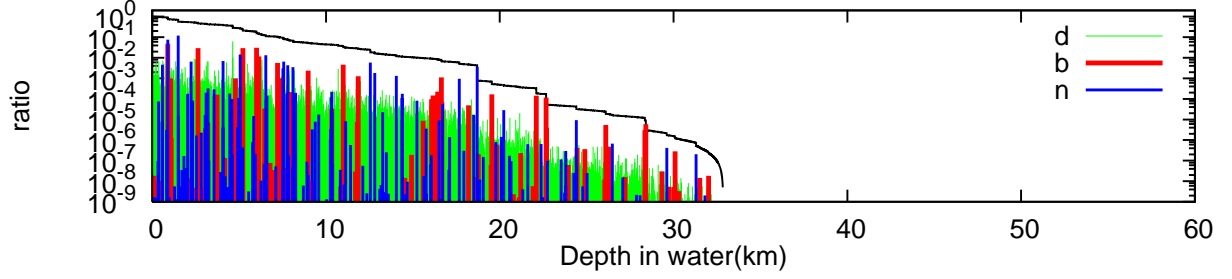


Figure 12: The fractional energy loss with *the average-like range* for 10^{18} eV muon together with the fractional energy of the muon.

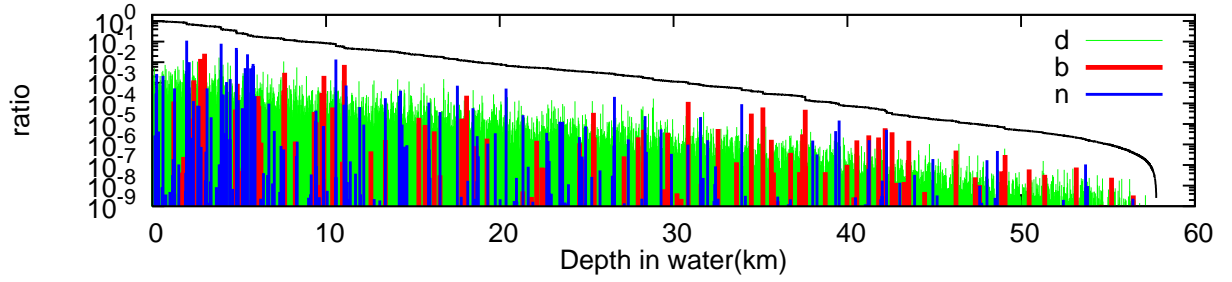


Figure 13: The fractional energy loss with *the longest range* for 10^{18} eV muon together with the fractional energy of the muon.

many energies in stochastic manner exactly, recording the locations of the interaction points for specified interactions and their dissipated energies exactly. However, we pursue the behaviors of all sam-

pled muons exactly, including three different types of the muons. We can construct the range distributions from ensemble of 100,000 individual muons for respective primary muon's energy, as shown in

Table 2: The ratios of energies transferred from bremsstrahlung, direct electron pair production and photonuclear interaction to the total energy loss (a) and their ratios expressed in respective average values (b).

E_0	Brems		Direct Pair		Nuclear	
	(a)	(b)	(a)	(b)	(a)	(b)
$E_0 = 10^{12} \text{eV}$						
<Average>	3.37×10^{-1}	1.00	5.26×10^{-1}	1.00	1.37×10^{-1}	1.00
Average-like	2.87×10^{-1}	0.872	4.30×10^{-1}	0.688	2.83×10^{-1}	2.51
Shortest	5.32×10^{-1}	2.96	3.76×10^{-1}	9.14×10^{-4}	9.20×10^{-2}	2.96×10^{-3}
Longest	3.50×10^{-2}	0.875	9.54×10^{-1}	1.33	1.10×10^{-2}	5.87×10^{-2}
$E_0 = 10^{15} \text{eV}$						
<Average>	3.40×10^{-1}	1.00	4.98×10^{-1}	1.00	1.62×10^{-1}	1.00
Average-like	7.54×10^{-1}	1.25	2.37×10^{-1}	0.960	9.36×10^{-3}	0.600
Shortest	8.66×10^{-1}	2.53	1.34×10^{-1}	0.178	5.90×10^{-5}	0.321
Longest	7.62×10^{-2}	0.541	8.11×10^{-1}	1.52	1.12×10^{-1}	0.364
$E_0 = 10^{18} \text{eV}$						
<Average>	3.24×10^{-1}	1.00	4.59×10^{-1}	1.00	2.17×10^{-1}	1.00
Average-like	1.68×10^{-1}	1.30	5.58×10^{-1}	0.858	2.74×10^{-1}	0.848
Shortest	8.75×10^{-1}	2.17	1.19×10^{-1}	0.634	6.23×10^{-3}	2.20×10^{-2}
Longest	5.71×10^{-2}	0.209	5.77×10^{-1}	1.49	3.66×10^{-1}	1.13

Fig.14. In the figure, we give $P(R; E_0)$, the probabilities for the range distribution in water with primary energies, 10^{12}eV to 10^{15}eV and 10^{18}eV in water whose minimum energy is 10^9eV (1GeV), respectively. It is clear from the figure that the width of the range distribution increases rapidly, as their primary energy increases. Also, as the primary energy decreases, the width of range distribution becomes narrower and approaches to a δ function-type, the limit of which denotes no fluctuation. It is interesting that the range distributions can be well approximated as the normal distribution above $\sim 10^{14} \text{eV}$ where the total Cherenkov light yields comes almost from the muon induced electromagnetic cascade showers and they are given as,

$$P(R; E_0) = \frac{1}{\sqrt{2\pi}\sigma} \exp\left(-\frac{R - \langle R \rangle}{2\sigma^2}\right), \quad (13)$$

, where E_0 , R , $\langle R \rangle$ and σ are primary energy, real range, the average value of ranges and the standard deviations, respectively. Their average ranges, standard deviations and relative variances (standard deviations divided by averages) in water are given in Table 3. Also, it is interesting that their relative variances decrease slightly as their primary energies increase. It should be noticed from Table 3 that the standard deviation increases as primary energy increases, but, the relative variance of the range distribution decreases inversely.

In order to examine each characteristic of the stochastic process, such as the bremsstrahlung, direct electron pair production and photonuclear interaction

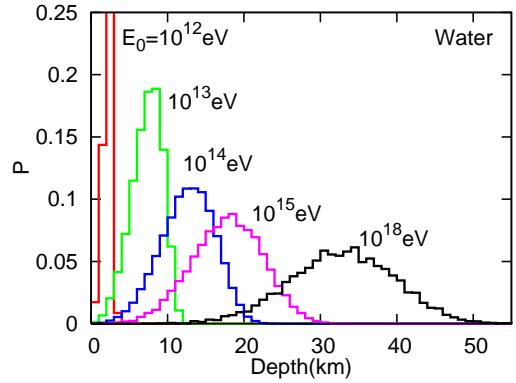


Figure 14: Range distributions for 10^{12}eV to 10^{18}eV muons in water. The minimum observation energies are taken as 10^9eV . Each sampling number is 100,000.

Table 3: The average values, the standard deviations and the relative variances of the range distributions of muons from 10^{11}eV to 10^{18}eV in water.

E_0 [eV]	$\langle R \rangle$ [km]	σ [km]	$\sigma / \langle R \rangle$
10^{11}	3.56×10^{-1}	2.52×10^{-2}	7.07×10^{-2}
10^{12}	2.43	4.71×10^{-1}	1.94×10^{-1}
10^{13}	7.28	2.02	2.78×10^{-1}
10^{14}	1.26×10^1	3.49	2.77×10^{-1}
10^{15}	1.78×10^1	4.57	2.57×10^{-1}
10^{16}	2.30×10^1	5.41	2.36×10^{-1}
10^{17}	2.79×10^1	6.14	2.20×10^{-1}
10^{18}	3.29×10^1	6.81	2.07×10^{-1}

teraction, we construct the hypothetical range distribution in which a specified stochastic process only is assumed to occur and the other two stochastic processes are assumed not to occur. To clarify the characteristics of the specified stochastic processes, we can compare this hypothetical range distribution with that of real range distribution in which every specified stochastic process is realized as the competition effect among these three processes. We compare the hypothetical range distribution with the real range distribution in Fig.15 to Fig.17.

In Fig.15, we compare three different hypothetical range distributions with the real range distribution for primary energy of 10^{13} eV. Here, the symbol **d** in these figures means the hypothetical range distribution in which only direct electron pair production is taken into account and both the bremsstrahlung and photo nuclear interaction are neglected. The symbols **b** and **n** have similar meaning to that of **d**. The symbol **t** means the real range distribution in which all interactions are taken into account (The true distribution). From the shapes of the distributions and their maximum frequencies for different stochastic processes in the figures, it is clear that energy losses in the direct electron pair production are of small fluctuation, while both the bremsstrahlung and photonuclear interaction are of bigger fluctuation, and the fluctuation in photonuclear interaction becomes bigger when compared with bremsstrahlung as primary energy increases. The smaller fluctuation in direct electron pair production suggests us that energy loss from this process may be treated as something like continuous energy loss in the special situation

2.5.4. Other physical quantities obtained from Time Sequential Procedure

In Fig.18 to Fig.20, we give the survival probabilities for different cutoff energies with primary energies of 10^{12} eV, 10^{15} eV and 10^{18} eV, respectively. The values for cutoff energies are given in respective figures. The sampling number utilized is 100,000 for each primary energy.

In Fig.21 to Fig. 23, we give the differential energy spectrum of muons for primary energies, 10^{12} eV, 10^{15} eV and 10^{18} eV, respectively. The energy spectrum of the survival muon obtained by *V_{cut} Procedure* is surmised to be different from that by *Time Sequential Procedure*, in particular, in higher energies. Their magnitude is smaller than that by *Time Sequential Procedure* and their shapes

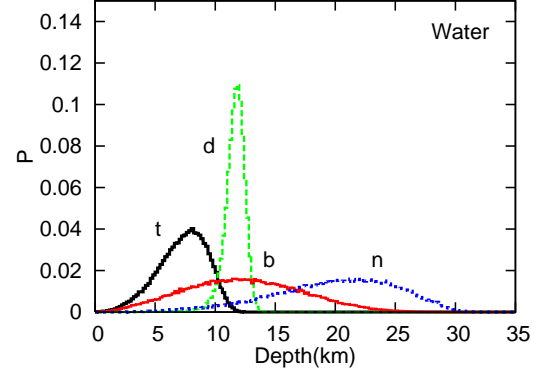


Figure 15: Hypothetical range distributions in water for 10^{13} eV muons together with the real range distribution.

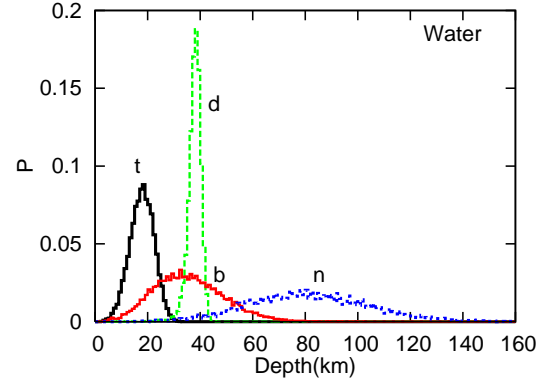


Figure 16: Hypothetical range distributions in water for 10^{15} eV muons together with the real range distribution.

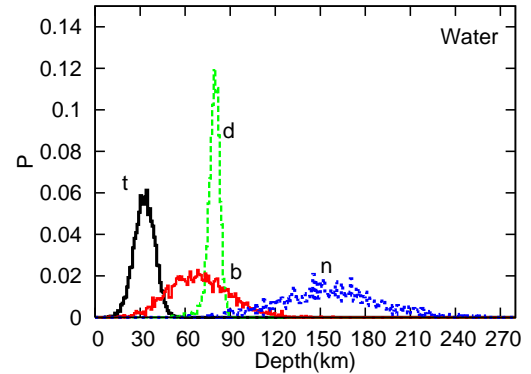


Figure 17: Hypothetical range distributions in water for 10^{18} eV muons together with the real range distribution.

are different from that by us. The reason for the difference is discussed briefly in the following section.

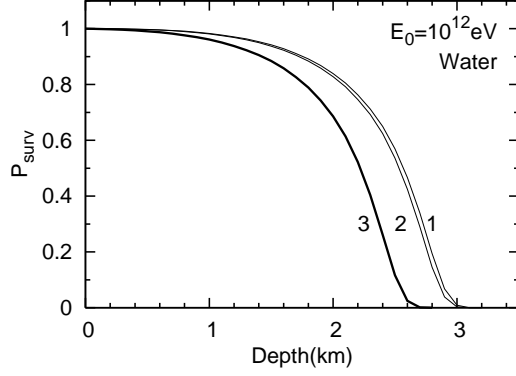


Figure 18: The survival probabilities for 10^{12} eV muon. Curves labels correspond to following set of cutoff energies: (1) 10^9 eV, (2) 10^{10} eV, (3) 10^{11} eV.

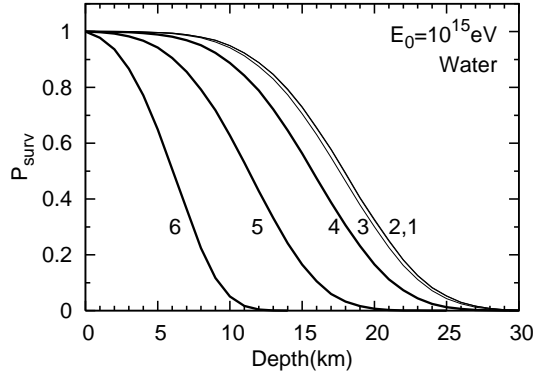


Figure 19: The survival probabilities for 10^{15} eV muon. Curves labels correspond to following set of cutoff energies: from (1) 10^9 eV to (6) 10^{14} eV.

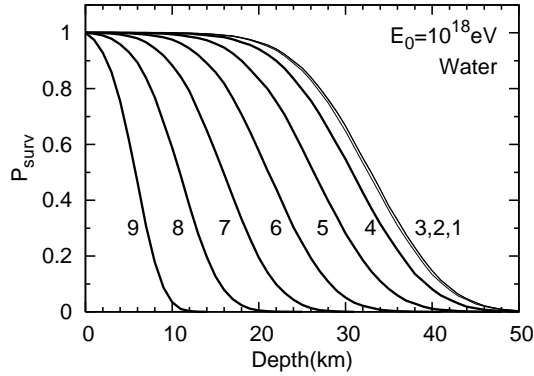


Figure 20: The survival probabilities for 10^{18} eV muon. Curves labels correspond to following set of cutoff energies: from (1) 10^9 eV to (9) 10^{17} eV.

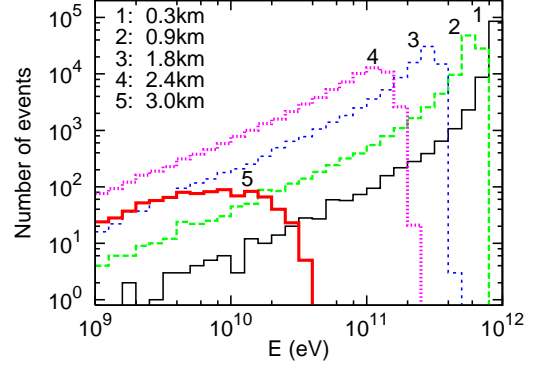


Figure 21: Energy spectrum in water at the different depths, initiated by 10^{12} eV muons.

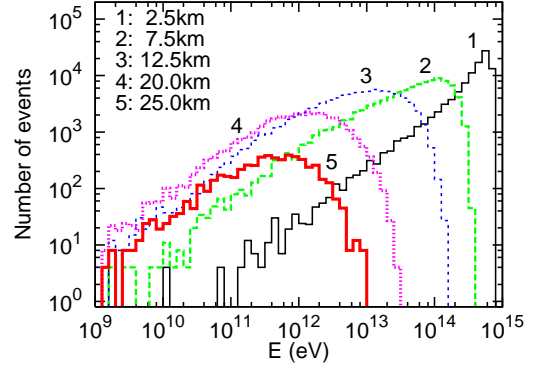


Figure 22: Energy spectrum in water at the different depths, initiated by 10^{15} eV muons.

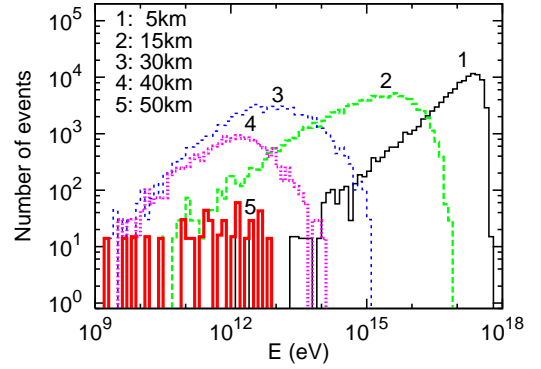


Figure 23: Energy spectrum in water at the different depths, initiated by 10^{18} eV muons.

3. V_{cut} Procedure: The fundamental structure and points at issue

3.1. V_{cut} Procedure as an approximated Time Sequential Procedure

Nobody has verified the validity of the logical structure of V_{cut} Procedure from the view point

of the fundamental idea of Monte Carlo method. The plausible reason why V_{cut} Procedure seems to give right results is simply that many people have utilized this technique and they obtain essentially same results. However, this does not always guarantee that V_{cut} Procedure is logically correct in the sense of Monte Carlo method, because it is quite natural for different authors to reach same results, if they utilize the same principle which, in same case, may be wrong. That is, the same results obtained by the Monte Carlo method due to different authors should be carefully examined in the spirit of Monte Carlo method.

As similarly in our examination (see, section 2.4), the validity of V_{cut} Procedure in the sense of Monte Carlo method should be examined by methodologically independent of Monte Carlo method, namely, by either analytical method or numerical one, focusing on the average values of several physical quantities⁴. It is rather easy to develop a numerical theory based on the same principle and compare the results obtained by the numerical theory with corresponding results obtained by V_{cut} Procedure. Here, we examine the fundamental structure of V_{cut} Procedure from a different point of view.

Lipari and Stanev [28] and subsequent authors, P.Antonioli, S.Iyer et al., Klimushin et al., D.Chirkin et al., S.Bottai et al. [29-34] formulate V_{cut} Procedure as follows:

$$\begin{aligned} \frac{dE}{dx} &= \left[\frac{dE}{dx} \right]_{soft} + \left[\frac{dE}{dx} \right]_{hard} \\ &= \frac{N}{A} E \int_0^{v_{cut}} dv \cdot v \frac{\sigma(v, E)}{dv} \\ &+ \frac{N}{A} E \int_{v_{cut}}^1 dv \cdot v \frac{d\sigma(v, E)}{dv}, \end{aligned} \quad (14)$$

, where v denotes the fractional emitted energy. They introduce v_{cut} , a certain constant value, into the diffusion equation, in such a way that the effective energy loss, for example, γ -ray above $v_{cut} \times E$, is treated in stochastically only *hard part*, while

⁴For example, in order to confirm the validity of the one dimensional Monte Carlo method for electromagnetic cascade shower, we should compare the averaged transition curves and/or track length for shower particles under Appo.A with the corresponding results obtained by the analytical theory. In three dimensional cases, the mean square of angular and lateral spreads for shower particles should be compared with each other for the validity of the Monte Carlo method [39-42].

that below $v_{cut} \times E$ is put into continuous energy loss (*soft part*), which is simply subtracted from the muons concerned.

Here, let us summarize the values of v_{cut} utilized in V_{cut} Procedure in the following. [a] Lipari and Stanev adopt $v_{cut} = 0.01$ [28], [b] Antonioli et al. adopt $v_{cut} = 10^{-3}$ [29], [c] Dutta et al. adopt $v_{cut} = 10^{-3}$ [31], [d] Sokalski et al. adopt $v_{cut} = 10^{-3}$ to 0.2 [32], [e] Chirikin and Rohde adopt $v_{cut} = 10^{-4}$ to 10^{-3} [32].

The problems to be involved into V_{cut} Procedure are as follows:

[A] It should be pointed that the separation of *soft part* from *hard part* is treated in inconsistent manner in V_{cut} Procedure as for fixed energy muon. Namely, the muon with the some energy is treated in *soft part* in some case, while the muon with the same energy is treated in *hard part* in another case. Such the treatment lack in consistency for description on muon behavior, because the effectiveness of fluctuation depends on the absolute values of muon energies.

V_{cut} Procedure pursues the change of energy state by step by step method with regard to the depth dx . Consequently, by the constancy of v_{cut} (10^{-4} under examination), their stochastic energy loss part (*hard part*) shifts toward lower energy region, as dx advances. In other words, as already mention, the muons with some energy belongs to *hard part* (stochastic energy loss part) at certain depth, but belongs to *soft part* (continuous energy loss part) at another depth, owing to the shift of the boundary line between *hard part* and *soft part*. Such a description on the behavior of the muon in V_{cut} Procedure clearly lack in consistency.

For example, comparing Fig.24(a) with Fig.24(b), it is clear that the region from 10^{14} eV to 10^{11} eV for $E_0 = 10^{18}$ eV belongs to *soft part*, while the same region belong to *hard part* for $E_0 = 10^{15}$ eV. This is also an example that the stochastic process is not treated in the unified manner.

On the contrast to V_{cut} Procedure, there are no separation of *soft part* from *hard part* in *Time Sequential Procedure* and only *hard part* exists. Namely, all plausible processes are treated in stochastic manner exactly in this procedure.

[B] For higher energy muons and/or larger v_{cut} , for example, in the case of bremsstrahlung, the emitted higher γ -rays may be contained in *soft part* in which they are subtracted from the muon concerned, being treated continuous energy loss and

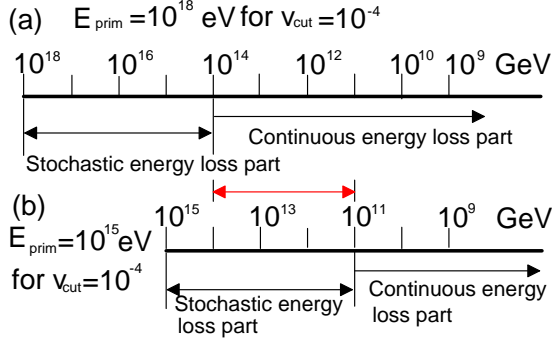


Figure 24: (a) The separation of stochastic energy loss part (*hard part*) from Continuous energy loss part (*soft part*) in the case $v_{cut} = 10^{-4}$ for 10^{18} eV. (b) The separation of stochastic energy loss part (*hard part*) from Continuous energy loss part (*soft part*) in the case $v_{cut} = 10^{-4}$ for 10^{15} eV

don't contribute to the muon's future behavior any more. However, some part of such the higher γ -rays may not be consumed as dissipated energies, if v_{cut} sets up more smaller. Then the muons concerned should maintain them in *hard part* and their energy loss may be treated in stochastic manner. As the result of it, the emitted γ -rays may be correctly taken into account in *hard part* so that the muon concerned can maintain higher energy than that in the case of larger v_{cut} and, consequently, more muons may survive than in the case of larger v_{cut} .

Namely, the present situation with larger v_{cut} in higher energies may induce smaller survival probability for the muon concerned. Thus, in the case of higher energy muons and/or larger v_{cut} , we expect the deformed high energy γ -rays (or electrons) spectrum, which, in turn, may result in the deformed Cherenkov light spectrum, compared with the most probable spectrum which can be obtained by *Time sequential Procedure*. This is inevitable problem, because these high energy γ -rays (electrons) spectrum are exclusively the sources of Cherenkov light in higher energies. (See, Conclusion and Outlook).

3.2. Comparison of the survival probabilities obtained by Time Sequential Procedure with those obtained by V_{cut} Procedure

In the previous section, we examine the inconsistency problems involved in V_{cut} Procedure. However, V_{cut} Procedure may be useful within their lim-

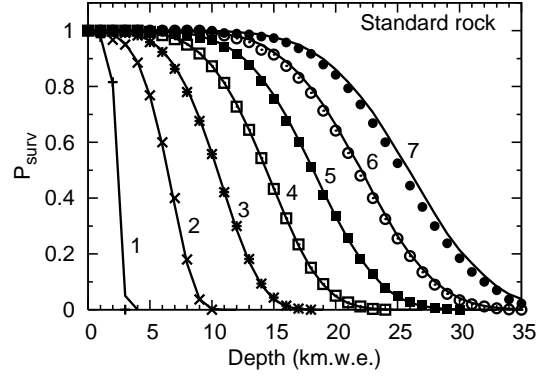


Figure 25: The comparison of our result with that of Lipari and Stanev[28]. The survival probabilities of muons of energy from 1 TeV to 10^6 TeV. The numerical figures attached each curve denote the primary energies. Curves labels correspond to following set of primay energies of muon: (1)1TeV, (2)10TeV, (3)10²TeV, (4)10³TeV, (5)10⁴TeV, (6)10⁵TeV, (7)10⁶TeV. Symbols are due to Lipari and Stanev and curves are due to ours.

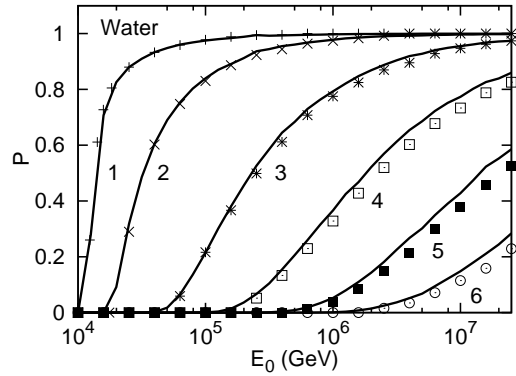


Figure 26: The comparison of our results with that of Klimushin et al[?]. The continuous lines are obtained by us, while symbols are readout from those by Klimushin et al for primary energies from 10^{13} eV to 3×10^{16} eV. The numerical figures attached each curve denote the threshold energy is 10 TeV. Curves labels correspond to following set of depths: (1)1.15km, (2)3.45km, (3)8.05km, (4)12.65km, (5)17.25km, (6)21.39km.

itation, because it may be regarded as an approximation of *Time Sequential Procedure*.

In Fig.25 and Fig.26, we give the comparison of our results by *Time Sequential Procedure* for survival probabilities with those of Lipari and Stanev and those of Klimushin et al. by V_{cut} Procedure, respectively. We discuss the agreement or disagreement between the results obtained by *Time Sequential Procedure* and V_{cut} Procedure. The agreement between Lipari and Stanev's (Fig.25) and ours is

quite well in the energies from 1 TeV to 10^4 TeV, while the disagreement between them become clear beyond 10^5 eV. As indicated in the beginning of [B], the γ -rays contained *soft part*, should be involved in the muon spectrum, if the stochastic processes concerned are taken into account. Therefore, this fact leads increase of survival probability and muon spectrum.

The agreement and disagreement between Klimushin et al's (Fig.26) can be explained similarly.

Also, it should be noticed that fluctuation effect depend entirely depend on the absolute values of muon's energy.

In V_{cut} Procedure, Monte Carlo procedure, the calculations are performed by step by step method in dx , which inevitably introduce uncertainties due to the accumulation effect in calculation error. One may call their procedure differential method. On the contrary to it, *Time Sequential Procedure* can determine interaction point directly (*integral method*). Consequently, its accuracy is independent of the errors coming from the accumulation effect coming from dx . One may call our procedure as *integral method* on the contrast to *differential method*.

4. Conclusion and Outlook

We have showed the validity of *Time Sequential Procedure* in the Monte Carlo method, through the comparison of our results with those obtained by the analytical theory which is methodologically independent. Also, we have examined the limitations for application imposed upon V_{cut} Procedure.

In KM3 detectors, we catch signals from Cherenkov light due to high energy muons. It should be emphasized here that Cherenkov light signal caught by KM3 comes exclusively muon induced electromagnetic cascade shower and the contribution from muon themselves is negligible.

Now, we discuss this problem in more detail. There are three different types of electromagnetic cascade showers among Cherenkov light which are produced from muon induced electromagnetic cascade shower. The first one is γ -ray induced electromagnetic cascade showers due to bremsstrahlung, the second is e^+ and e^- induced electromagnetic shower due to direct electron pair production and the third is $\pi_0 - 2\gamma$ induced electromagnetic cascades showers due to photonuclear interaction. In

our procedure, the electromagnetic cascade showers are also exactly simulated which are origins of Cherenkov light.

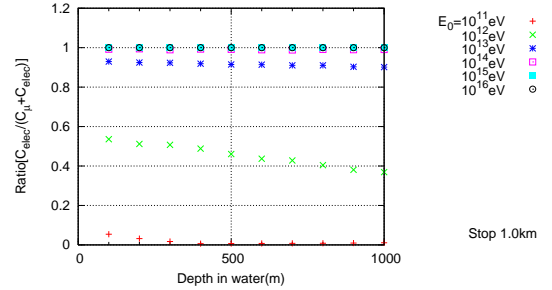


Figure 27: Ratio of Cherenkov lights due to the accompanied cascade showers to the Cherenkov light.

In Fig.27, we give the ratios of Cherenkov light due to muon induced electromagnetic cascade showers to the total Cherenkov light as the function of the depth traversed for 10^{11} eV to 10^{16} eV. It is clear from the figure that $\sim 10^{11}$ eV, the most of Cherenkov light comes from muon itself, while above 10^{14} eV the most Cherenkov light comes from the muon induced electromagnetic cascade showers and, consequently, Cherenkov light from the original muon is completely negligible. Just this situation around Cherenkov light production strongly imposes the limit for application of V_{cut} Procedure to estimation of the energy of muon events in KM3 detectors.

Thus, the origins of the electromagnetic cascade shower are either γ -ray (in the case of bremsstrahlung and photonuclear interaction) or electrons (in the case of direct electron pair production) and, consequently, in order to obtain Cherenkov light yield correctly, it is necessary to know the behaviors of electromagnetic cascade showers due to different stochastic processes which are sources for Cherenkov light and, furthermore, to know the energy spectrum of 'primary' electron and γ -ray which are the origins of electromagnetic cascade showers. In *Time Sequential Procedure*, we exactly the muon behaviors in stochastic manner, without introducing *soft part* and, consequently, we obtain accurate muon energy spectrum at arbitrary depths as well as the energy spectrum of 'primary' (in the sense of origin of electromagnetic cascade showers) electrons and γ -rays at arbitrary depths. However, in V_{cut} Procedure, one cannot obtain accurate 'primary' electrons and γ -ray energy spectrum

due to strong limitation involved in their technique, which is examined in section 3. In particula, the emitted energies from *soft part* are difficult to handle accurately for higher muon energies and rather larger v_{cut} in *V_{cut} Procedure*.

Thus, it is rather easily concluded that, compared with *Time Sequential method*, *V_{cut} Procedure* involve the difficulty around accurate muon energy spectrum, but also 'primary' γ -rays and electron energy spectrum which are sources of Cherenkov light, which may distort finally the fluctuation effect in Cherenkov light.

Now, our discussion still remains to single high energy muon problem. However, really, muon does not exist singly, but they exist in the form of energy spectrum which is directly reflection of parent neutrino spectrum. The existence of energy spectrum of muons brings more difficulty into the elucidation of fluctuation effect even in *Time Sequential Procedure*. These effects intermingle with each other and we could not discuss them separately. However, it can be technically overcome in *Time Sequential Procedure*, while, in principle, it seems to be almost difficult to be solved in *V_{cut} Procedure*.

Up to now, we restrict our discussion around electromagnetic cascade shower to Bethe-Heitler shower. However, we could not neglect LPM effects, related to the interpretation of extremely high energy muon events in future. One is related to electrons [42-47] and other is related to muon [48,49]. We cannot neglect the LPM effect on the behaviors of electromagnetic cascade themselves above $\sim 10^{15}$ eV in Water [45]. However, the LPM effect is supposed to be effective above 10^{18} eV in the case of muon induced electromagnetic cascade showers.

In such extremely high energies, range fluctuation of muon may alter their feature essentially compared with that of present situation. Furthermore, above 10^{21} eV, we cannot neglect the LPM effect related to the muons [48,49]. Namely, above 10^{21} eV, Cherenkov light spectrum is supposed to become essentially different from those in the absence of two kinds of LPM effects at present.

In the present paper, we restrict our discussion to muons themselves in high energies. In subsequent papers, we will extend our discussion Cherenkov light yield via electromagnetic cascade showers from different interactions, such as, bremsstrahlung, direct electron pair production and photonuclear interaction, taking into account of muon energy spectrum for imaging KM3 detector. Here, main subject will be the discussion of Cherenkov light yield

from muon induced electromagnetic cascade showers.

In discussion of the problems around high energy neutrino spectrum from the universe, it should be noticed that the reliable results are obtained only through the utilization of the stochastically correct tools, taking into account of very few number of experimental events, in addition to strong steepness of high energy neutrino spectrum.

Acknowledgments

One of authors (A.M.) would like to express his thanks to The Institute for China-Japan Culture Study for providing the research fund and for stimulating him.

References

- [1] M.G.K.Menon, P.V.Ramana Murthy, Progress in Elementary Particles and Cosmic Ray Physics, Vol.9 (1967) 161-243, North- Holland Publ.
- [2] Y.Miyazaki, Phys. Rev. **76** (1949) 1733
- [3] S.Miyake, V.S.Narashimham, P.V.Ramana Murthy, Nuovo Cimento **32** (1964) 1505
- [4] E.V.Bugaev, A.Misaki, V.A.Naumov, T.S. Sinogovskaya, S.I.Sinogovskiy, N.Takahashi, Phys. Rev. D **58** (1998) 054001
- [5] <http://baikalweb.jinr.ru/>
- [6] <http://icecube.wisc.edu/>
- [7] <http://antares.in2ps.fr/>
- [8] <http://nemoweb.lns.infn.it/>
- [9] M.Mand, L.Ronchi, Nuovo Cimento **9** (1952) 105
- [10] M.Mand, L.Ronchi, Nuovo Cimento **9** (1952) 517
- [11] M.Mando, P.G.Sona, Nuovo Cimento **10** (1953) 1275
- [12] I.L.Rozental, V.N.Streltsov, Zh.Eksp. Teor. Fiz **35** (1958) 1440
- [13] G.T.Zatsepin, E.D.Mikhailchi, Proc. 0th Int. Cosmic Ray Conf., Kyoto, Japan **3** (1961) 356
- [14] J.Nishimura, Proc. 8th Int. Cosmic Ray Conf., Jaipur, India **6** (1963) 224
- [15] V.I.Gurentsov, G.T.Zatsepin, E.D.Mikhailchi, Sov.Jour.Nuc.Phys. **23** (1976) 527
- [16] K.Kobayakawa, Nuovo Cimento B **47** (1967) 156
- [17] A.Misaki, J.Nishimura, Uchusen Kenkyuu **21** (1976) 250; ICR-Report-45774-4, University of Tokyo (1977)
- [18] V.I.Gurentsov, G.T.Zatsepin and E.D. Mikhailchi, Sov.J.Nucl.Phys. **23** (1976) 527
- [19] Y.Minorikawa, T.Kitamura, K.Kobayakawa, Nuovo Cimento C **4** (1981) 471
- [20] H.Oda, T.Murayama, Jur.Phys.Sos.Japan **20** (1965) 1549
- [21] H.J.Bolinger, Ph.D thesis, Cornel University (1958)
- [22] P.J.Hayman, A.W.Wolfendale, Proc. Phys. Soc. **80** (1962) 710
- [23] P.J.Hayman, N.S.Palmer, A.W.Wolfendale, Proc. Roy. Soc. A **275** (1963) 391
- [24] P.V.Ramana Murthy, Ph.D thesis, Bombay University (1962)

- [25] S.Miyake, V.S.Narasimham, P.V.Ramana Murthy, Nuovo Cimento **32** (1964) 1524
- [26] N.Takahashi, A.Misaki, A.Adachi, N.Ogita, Y.Okamoto, K.Mitsui, H.Kujirai, S.Miono, O.Saavedra, Proc.18th Int. Cosmic Ray Conf., Bangalore, India **11** (1983) 443
- [27] N.Takahashi, H.Kujirai, A.Adachi, N.Ogita, A.Misaki, Uchusen Kenkyuu **28** (1984) 120
- [28] P.Lipari, T.Stanev, Phys. Rev. D **44** (1991) 3543
- [29] P.Antonioli, C.Ghetti, E.V.Korolkova, V.A. Kudryavtsev, G.Sartorelli, Asroparticle Physics **7** (1997) 357
- [30] S.Bottai, L.Perrone, Nucl.Instrment and Method in Research A **459** (2001) 319
- [31] S.Iyer Dutta, M.H.Reno, I.Sarcevic, D. Seckel, Phys.Rev. D **63** (2001) 094020
- [32] S.I.Klimushin, E.V.Bugaev, I.A.Sokalski, Phys. Rev. D **64** (2001) 014016
- [33] L.A.Sokalski, E.V.Bugaev, S.I.Klimushin, Phys. Rev. D **64** (2001) 074015
- [34] D.Chirkin, W.Rhode, hep-ph 0407075 v2 (2008)
- [35] For example, S.R.Kelner, R.P.Kokoulin, A.A. Petrukhin, Preprint MEPHI 024-95 Moscow (1995); CERN SCAN-9510048
- [36] For example, R.P.Kokoulin, A.A.Petrukhin, Proc. 11st Int. Cosmic Ray Conf., Budapest, Hungary MU-**41** (1969) 277
- [37] For example, V.V.Borog, A.A.Petrukhin, Proc. 14th Int. Cosmic Ray Conf., Munchen, Germany **6** (1975) 1949
- [38] M.Tamura, Prog.Theor.Phys. **34** (1965) 912
- [39] B.Rossi, K.Greisen, Rev.Mod.Phys. **13** (1941) 240
- [40] J.Nishimura, Handbuch der Physik, **XLVI/2**, 'COSMIC RAY II', Springer-Verlag, (1966) 1
- [41] A.Misaki, Suppl.Prog.Theor.Phys., Suppl. Theor.Phys. **89** (1965) 82
- [42] Konishi, A.Misaki, N.Fujimaki, Nuovo Cimento, **44 A** (1978) 509
- [43] T.Stanev, Ch.Vankov, R.E.Streitmatter, R.W. Ellsworth, T.Bowen, Phys. Rev. D **25** (1982) 1291
- [44] E.Konishi, A.Adachi, N.Takahashi, A.Misaki, J.Phys.G:Nuc.and Part.Phys., **17** (1991)719
- [45] A.Misaki, Fort.Schr. d. Phys. **38** (1990) 413
- [46] A.Misaki, Nuov.Cim. **13 C** (1990) 733
- [47] A.Misaki, Phys. Rev. D **40** (1990) 3086
- [48] S.Polytiko, M.Kato, E.Konishi, N.Takahashi, A.Misaki, J.Phys.G:Nucl.and Part.Phys. **28** (2002) 427
- [49] S.Polytiko, N.Takahashi, M.Kato, Y.Yamada, A.Misaki, Nucl. Instr. Meth. in Physical Research B **173** (2001) 30